OENO One
VINE AND WINE OPEN ACCESS JOURNAL
By iVES International Viticulture & Enology Society

DOI: https://doi.org/10.20870/oeno-one.2023.57.2.7243

OPEN ACCESS

ORIGINAL RESEARCH ARTICLE

Interaction between Armenian clay-based ceramics and model wine during storage

Syuzanna Esoyan[1,2], Camille Loupiac[1], Nelli Hovhannisyan[2], Régis D. Gougeon[3], Thomas Karbowiak[1], Bernhard Michalke[4], Philippe Schmitt-Kopplin[4,5], Claude Fontaine[6], Sabine Valange[6] and Philippe R. Bodart[1]*

[1] Université Bourgogne Franche-Comté, Institute Agro Dijon, UMR PAM A02.102, 1 Esplanade Erasme, 21000, Dijon, France
[2] Yerevan State University, Institute of Biology, 1 Alex Manoogian Str., 0025, Yerevan, Armenia
[3] Institut Universitaire de la Vigne et du Vin, UMR PAM A02.102, Université Bourgogne Franche-Comté, Esplanade Erasme, 21000, Dijon, France
[4] Research Unit Analytical BioGeoChemistry, Helmholtz Zentrum München, Ingolstädter Landstraße 1, 85764, Neuherberg, Germany
[5] Technische Universität München, Analytical Food Chemistry, Alte Akademie 10, 85354, Freising-Weihenstephan, Germany
[6] Institut de Chimie des Milieux et Matériaux de Poitiers (IC2MP), Université de Poitiers, CNRS, UMR 7285, ENSI Poitiers, B1, 1 rue Marcel Doré, 86073 Poitiers Cedex 9, France

ABSTRACT

Wine made or stored in clayware ceramic pots attracts the attention of consumers, but this practice is less studied than when classic stainless steel tanks or wood barrels are used. It is known that wine can be influenced by the container in which it is aged. To analyse the influence of ceramics on the chemical composition of wine, Armenian clay-based ceramic tablets were immersed in model wine and aged from 1 hour up to 16 months at 25 °C in darkness. The concentrations of 26 elements (namely: Al, B, Ba, Be, Ca, Cd, Co, Cr, Cu, Fe, Hg, K, Li, Mg, Mn, Mo, Na, Ni, P, Pb, S, Sr, Ti, V, W and Zn) in 19 samples were determined by ICP-AES analysis. Proton time domain NMR relaxometry was used to characterise the iron redox processes that occurred in the model wine in contact with a ceramic. A fast increase in the pH of the model wine in contact with the bare ceramic tablet (from 2.35 to 5) was recorded in 4 days. The coating of the ceramic tablets with beeswax showed a significant effect on the interaction between the model wine and the ceramic.

KEYWORDS: clayware ceramic containers, wine-ageing, interactions, ICP-AES, Time domain NMR relaxometry

*correspondence:
philippe.bodart@u-bourgogne.fr

Associate editor:
Valeriu Cotea

Received:
2 November 2022

Accepted:
6 April 2023

Published:
4 May 2023

This article is published under the **Creative Commons licence** (CC BY 4.0).

Use of all or part of the content of this article must mention the authors, the year of publication, the title, the name of the journal, the volume, the pages and the DOI in compliance with the information given above.

INTRODUCTION

The use of ceramic vessels has a history of tens of millennia. These vessels were most likely used to store and transport water, various types of liquids, grain and other foods, and later wine (Twede, 2002). MacNeil (2015) mentions ceramic jars as one of the earliest vessels for transporting wine in the ancient world. Archaeological excavations in the Armenian highlands have discovered winemaking complexes (in Adablur, Karmir Blur, Areni and other sites), which describe the primary phases and patterns of wine production. Of particular importance are the hundreds of grape sprouts, barks, fruit stems, seeds, pressed fruits and pulp remains discovered in the Areni-1 cave in the Vayots Dzor Province of Armenia, as well as the oldest known wine-producing facility, which is at least 6000 years old (Hovhannisyan *et al.*, 2017). Over the centuries, ceramic pots gradually gave up their place, both for transport or storage and for vinification, to other types of containers like oak barrels, concrete and stainless steel tanks and glass containers. However, ceramic pots remained a container of choice in countries such as Armenia and Georgia, but they are also used to some extent in Greece, Italy, France and Portugal (Harutyunyan *et al.*, 2022; Hovhannisyan *et al.*, 2017; McGovern *et al.*, 2017). Nowadays, there is a growing interest in using ceramics for wine production due to the popular natural wine movement, which practices traditional, even ancient, winemaking techniques. Despite this interest, there are few analytical studies about the interaction between ceramic containers and wine, in particular concerning the migration of elements from the ceramic to the wine (Shackelford and Shackelford, 2020; Weltman, 2018).

Ceramic pots, like concrete tanks and wood (mainly oak) barrels, are known for their porous structure. It makes them favourable for oxygen transfer which plays an important role from the perspective of oxidative ageing (Work, 2014). Unlike stainless steel, wood barrels, ceramic pots and concrete tanks are thermally stable due to lower thermal conductivity (0.17 $Wm^{-1}K^{-1}$; 0.5 $Wm^{-1}K^{-1}$; 20.5 $Wm^{-1}K^{-1}$ for oak, concrete and stainless steel, respectively) and the thickness of their walls, which makes them stable to temperature fluctuations (Gil i Cortiella *et al.*, 2021; Montalvo *et al.*, 2021). Stainless steel and glass containers can claim to be the most flavour-neutral containers, being chemically stable, thus, preserving the flavour and aroma properties of wine, producing a more stable and homogenous wine (Gil i Cortiella *et al.*, 2021; Montalvo *et al.*, 2021). Opinions on flavour neutrality are not consensual for concrete tanks and ceramic pots, particularly if they are not coated (e.g., with epoxy paint for concrete (Montalvo *et al.*, 2021), beeswax (Barisashvili, 2011; Johnson *et al.*, 2013), or pine pitch for ceramic (Romanus *et al.*, 2009). Wood barrels stand out for their influence on wine flavour. When interacting with wood, the wine is enriched with a remarkable diversity of phenolic and aromatic compounds from the wood, thereby influencing the organoleptic profile and increasing the antioxidant stability (oak barrels) of the wine (Gougeon *et al.*, 2009; Martínez-Gil *et al.*, 2022; Nikolantonaki *et al.*, 2019).

Summarising the available information on the interactions between containers and wine, we can state that, in contrast to the influence of wood barrels on the physicochemical and organoleptic (texture and taste) properties of wine, which has been widely studied, the effects of alternative containers are poorly studied, and little is known about their impact on the chemical composition of the resulting wines (Cabrita *et al.*, 2018; Gil i Cortiella *et al.*, 2021; Guerrini *et al.*, 2022). However, it can be said with confidence that the type of tank material plays an important role in directly impacting the quality, taste, and characteristics of wines. Wood and ceramic containers provide micro-oxygenation of wine thanks to their porous structure. Wood barrels are also a source of extra tertiary aromas. Stainless steel tanks allow for keeping the natural taste and aromas of the wine (Gil i Cortiella *et al.*, 2021; Nevares and del Alamo-Sanza, 2021).

The main objective of this study is to characterise the interactions between Armenian clay-based ceramics and model wine in terms of wine composition and redox processes occurring during ageing. Quantification of the elements present in the model wine was determined by inductively coupled plasma atomic emission spectroscopy (ICP-AES). Iron redox processes were investigated by ^{1}H time-domain NMR (TD NMR).

MATERIALS

1. Clay-based ceramics

The ceramic tablets (Figure 1) used for the experiments were prepared by mixing clay and sand (seeds smaller than 4 µm) in a ratio of 2:1, respectively. Armenian clay from Shahumyan village (chemical compositions of two samples of clay deposit and one sample of body clay (mixture of clay/sand (2:1) and water) reported in Figure 2 and detailed in Supplementary data, Table S1) was used as the starting material for the elaboration of ceramic tablets. The tablets were shaped cylindrically using a homemade plastic extruder. After shaping, the tablets were air-dried at room temperature for 3 days. The firing protocol is composed of three steps. The first step involves heating the samples for 4 hours from ambient temperature (20 °C) to 600 °C (2.4 °C/min). The second step is a fast temperature increase from 600 °C to 930 °C (20 °C/min) followed by firing at 930 °C for 2 hours. The final step is free cooling in the furnace. This firing protocol mimics the technique used in Armenia to produce such jars (arm. կարաս [karas]).

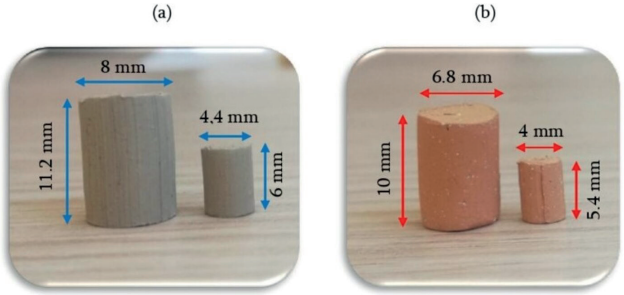


FIGURE 1. The tablets and their average dimensions before (a) and after (b) heat treatment

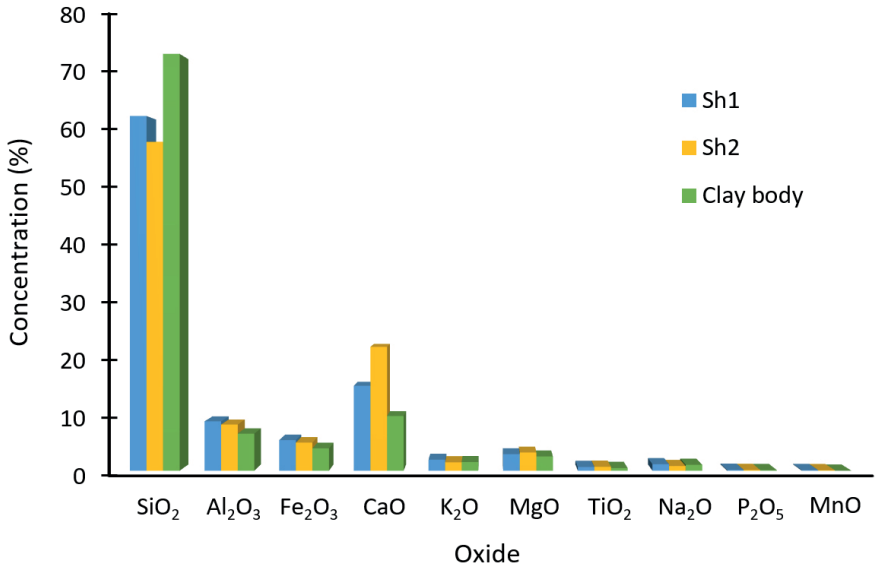


FIGURE 2. Representative histogram of XRF analyses

2. Model wine

The composition of the model wine consisted of 5 g/L tartaric acid (Sigma Aldrich ≥ 99.7 %, Marck KGaA 64271 Darmstadt, Germany) and 12 % (v/v) ethanol (Sigma Aldrich ≥ 99.9 %, Marck KGaA 64271 Darmstadt, Germany) dissolved in ultrapure water (VWR, LS-MS grade, VWR, LiChrosolv, Marck KGaA 64271 Darmstadt, Germany). The pH of the solution was 2.3–2.4, which is the natural pH of 5 g/L tartaric acid solution, a bit lower than expected in wine. Elemental analysis revealed a number of elemental impurities (Supplementary data, Table S1). Their concentrations were systematically subtracted from the ICP-AES analyses of the model wine in contact with the ceramics.

3. Beeswax

The beeswax was provided in the form of a natural comb without foundation by a beekeeper; the wax was a few days old that had not yet been used by bees (for eggs or honey deposits). The beeswax was used as received. Covering was performed by a two-step immersion of the ceramic tablet in melted beeswax (~70 °C). One half of the ceramic tablet was immersed for a few seconds, then removed and allowed to cool, and then the other half of the ceramic was immersed. These operations were repeated twice when two layers of beeswax were used. About 16 mg of beeswax was used to coat the tablet with one layer and 75 mg for the two-layer coating. Experiments with beeswax alone (no ceramic tablet) were performed with 5 mg of beeswax. Two replicates were performed for each sample.

METHODS

1. Mineralogical analysis of the ceramics

The mineralogical composition of the ceramics was identified by X-ray diffraction. A D8 Advance diffractometer (Bruker, Karlsruhe, Germany), equipped with a copper anticathode (radiation $\lambda \mathrm{Cu}K_\alpha$= 1.541838 Å after filtering through a nickel blade), mounted in θ/θ Bragg–Brentano configuration was used. Approximately 500 mg of powder homogenised with agate mortar was placed on hollowed-out support and analysed at 40 kV and 40 mA. Scans were recorded in the 2.5–65° 2θ range with a step time of 45 s/2° 2θ. The diffractograms were processed with HighScore software and phase identification was performed by comparison with the information of the JCPDS ICDD PDF-3 database.

2. BET characterisation of the ceramics

The specific surface area of the ceramic tablets was determined by adsorption-desorption of nitrogen on an ASAP2020 Micromeritics instrument (Micromeritics, Unterschleissheim, Germany) (T = –196 °C) using the Brunner–Emmett–Teller (BET) method. The samples (5 large ceramic tablets with a mass of about 5 g) were degassed under vacuum (P ≤ 0.7 Pa) at 350 °C for 4 hours prior to measurements.

3. Elemental analysis of model wine

3.1. Experimental setup

Nineteen samples were prepared for analysis (one sample with the model wine alone and 18 samples with the ceramic tablet in contact with the model wine). For each sample, one ceramic tablet was placed in a 10 mm NMR tube, then a neck was shaped (with a flame) in the middle of the tube, and finally, 2.8 mL of model wine was added, after which the tube was flame sealed. The ratio of the volume of model wine to headspace volume (V_{hs}/V_{wine}) was around 1:3. In the sealed tubes, in a controlled environment, the model wine was left in contact with the ceramic from 1 hour up to 16 months. All samples were stored at 25 °C during the first day in a water bath, with moderate exposition to the natural light of the laboratory, then in a regulated thermal (25 °C) chamber in darkness. The neck in the middle of the NMR tube allowed a simple reversal to separate the ceramic tablet from the model wine; it also allowed us to flame seal the two halves without opening the tube (the ratio V_{hs}/V_{wine} was less than 1:2).

Each model wine sample was stored at 25 °C in darkness until the last ageing period (16 months for the last sample) had elapsed. Eventually, all model wine samples were chemically analysed by ICP-AES at the same time.

3.2. Inductively coupled plasma atomic emission spectroscopy

Elemental analyses of the model wines after contact with the ceramic were performed using an ICP-AES Spectro ARCOS system (SPECTRO Analytical Instruments GmbH & Co. KG, Kleve, Germany). 26 elements (namely: Al, B, Ba, Be, Ca, Cd, Co, Cr, Cu, Fe, Hg, K, Li, Mg, Mn, Mo, Na, Ni, P, Pb, S, Sr, Ti, V, W and Zn) were investigated. Sample introduction was carried out using a peristaltic pump connected to a Meinhard nebuliser with a cyclone spray chamber. The RF power was set to 1250 W, and the plasma gas was 15 L Ar/min, whereas the nebuliser gas was 0.6 L Ar/min. Table 1 shows the wavelengths used for the determination of elements (Aceto *et al*., 2002; Ohls and Bogdain, 2016).

TABLE 1. Wavelengths used for determination of elements with ICP-AES.

Element	ICP-AES (λ) (nm)	Element	ICP-AES (λ) (nm)
Al	396.152	Mg	279.553
B	249.773	Mn	257.611
Ba	455.403	Mo	202.03
Be	313.042	Na	589.592
Ca	317.933	Ni	231.614
Cd	214.438	P	214.914
Co	228.616	Pb	220.353
Cr	267.716	S	182.036
Cu	324.754	Sr	407.771
Fe	259.941	Ti	334.941
Hg	194.164	V	292.402
K	769.869	W	207.911
Li	670.784	Zn	213.856

4. TD NMR analysis of the model wine in contact with the ceramics

4.1. Experimental setup

Proton time domain analysis was carried out on two types of samples (with beeswax-coated or non-coated ceramic tablets). For both types of samples, the experimental design was identical: a closed NMR tube containing 500 µL (non-coated ceramic) or 700 µL (beeswax-coated ceramic) of model wine was equipped with a home-made system allowing a gentle insertion of the ceramic into the wine. Measurements were performed continuously. After a few measurements of the model wine alone, the ceramic was delicately immersed in the model wine without stopping the measurement. The ratio V_{hs}/V_{wine} was 17 and 12 for coated and non-coated ceramic tablets, respectively.

4.2. Time domain nuclear magnetic resonance

Proton time domain NMR measurements were performed to characterise the processes occurring in the model wine in contact with the ceramic through spin-lattice (longitudinal) relaxation processes (T_1). Low-field NMR experiments were recorded at 25 °C on a minispec mq20 (Bruker, Karlsruhe, Germany), operating at 19.65 MHz. Longitudinal relaxation times were measured with an inversion recovery pulse sequence. The 90° and 180° pulse lengths were set to 2.8 µs and 4.4 µs, respectively. The recycling delay was set to 6 times T_1. Sixteen points were recorded for building the relaxation curves. For each acquisition, four scans were collected. The total measuring time varied from 10 to 20 min. Hereafter, we call the results of the TD NMR experiments reporting the evolution of the relaxation rate in function of the time: relaxograms (Bodart *et al.*, 2022; van Duynhoven *et al.*, 2010).

RESULTS AND DISCUSSION

To study the interaction of ceramics with model wine, we choose to insert a piece of ceramic (Figure 1) into the model wine instead of studying the ageing of the model wine into a ceramic vessel. The principal reasons are (i) the scale of the experiments involved if real containers have to be used, which prevents in situ experiments, (ii) the impact of the stopper (e.g., ceramic plate sealed with beeswax) and (iii) the reproducibility issues, and the additional complexity of the data analysis (due to the impact of an external surface in contact with atmosphere or soil (if buried). Therefore, this study focuses on the interaction of the internal surface of a ceramic vessel in contact with the wine, removing the impact of the external surface (e.g., dioxygen migration through the ceramic). To compare with a real situation, besides the headspace volume, one critical dimension in this study is the hydraulic ratio of the ceramic that we consider by the ratio of the wine volume over the surface of the ceramic ($R_{V/S}$).

1. Characterisation of ceramics by XRD and BET

The mineralogical composition of ceramics was determined by X-ray diffraction. A representative diffractogram (Supplementary data, Figure S1) shows that ceramic is mainly constituted of quartz (3.34 Å) and calcium silicate minerals, such as plagioclase (3.18 Å) of the albite–bytownite sequence ($Ca_{0.8}Na_{0.2}(Al_{1.6}Si_{2.4})O_8$), diopside (2.99 Å) ($CaMgSi_2O_6$), gehlenite (2.86 Å) ($Ca_2Al(AlSi)O_7$), along with hematite (2.69 Å). The presence of hematite (Fe_2O_3) can be considered as a reservoir of iron which can catalyse wine oxidation (Cacho *et al*., 1995; Coleman *et al*., 2020; Danilewicz, 2016; Danilewicz, 2018; Elias and Waterhouse, 2010).

The specific surface area of the ceramic tablets measured by the BET method was 2 m^2/g, which qualifies these ceramics as low porous materials. Remarkably, the same measurement on a fragment of Armenian pithos (degassed at 600 °C) gave a close value of 2.2 m^2/g.

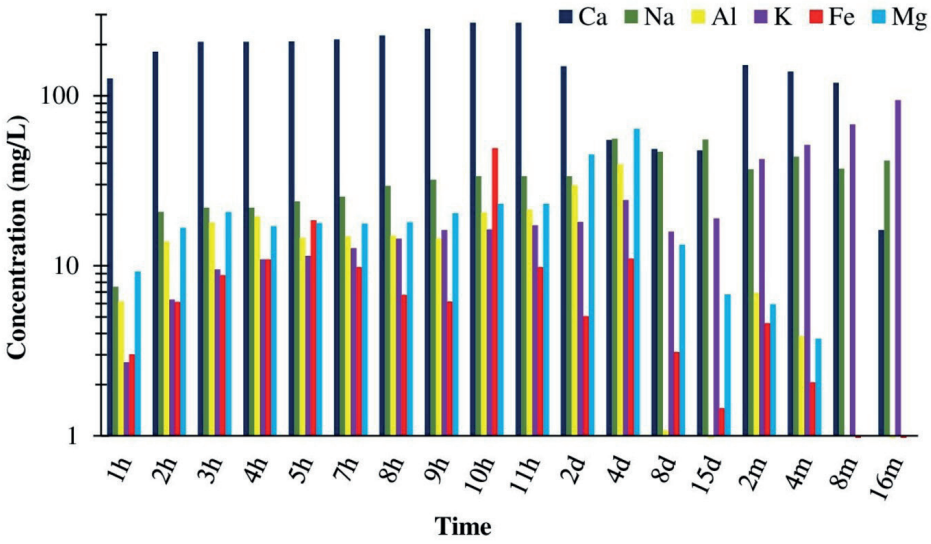


FIGURE 3. Concentrations (log scale) of the six most abundant elements released from 1 g of ceramic tablet in contact with the model wine. The contact time varies from 1 h (1 hour) up to 16 m (16 months); on the x-axis, d stands for days. The concentrations of elements in the model wine were subtracted.

2. Elemental composition of model wine in contact with a ceramic determined by ICP-AES

2.1. Elements migration and pH evolution

When the model wine is in contact with the ceramic, significant migration of elements from the ceramic to the model wine is observed (Figure 3) (complete ICP-AES data are compiled in the Supplementary data, Table S3). It should be noted that the migration behaviour of elements changes over time, but if we try to rank the most abundant elements, a list could be ordered as follows: Ca>>Na>Al>K>Fe>Mg>S>Sr. Compared to the other elements, from the first instants, calcium stands out with an obviously high concentration (up to 193 mg/L, 4.8 mM, after 11 hours). Overall, the concentrations seem to evolve with at least three-time scales: hours, days and months. For most elements, there is a fast release during the first few hours, and then the rate decreases. From there, three rough trends of evolution can be suspected: (i) a decrease after 4 days (Al, Mg, Fe); (ii) a rather steady state situation at a constant level over 16 months (Na, S); (iii) an increase over a long time period (K, Cr).

Simple principles of liquid chemistry were used to approximate the evolution of the dominant element Ca, which concentration evolution is reported in Figure 4. The raw clay contains a lot of calcite ($CaCO_3$) (~15–20 % w/w in the clay and ~10 % in the clay/sand mixture, Figure 2 and Table S1 in Supplementary data). We assume that calcite is the main raw source of calcium that migrates into the model wine. Upon firing, calcite forms calcium oxide (CaO) (Nikulshina *et al.*, 2007; Sanchez-Garmendia *et al.*, 2021; Stanmore and Gilot, 2005), which is also expected to be significantly present in the ceramic.

$$CaCO_3 \xrightarrow{\sim 800\,^{\circ}C} CaO + CO_2. \qquad (1)$$

The calcium oxide reacts rapidly with liquid water (when exposed to wine and probably also, to a lesser extent, with atmospheric water during storage of the ceramic) to form calcium hydroxide ($Ca(OH)_2$) (Criado *et al.*, 2014; Serris *et al.*, 2011).

$$CaO + H_2O \rightarrow Ca(OH)_2. \qquad (2)$$

This hydroxide is known to be slightly soluble in water (~1.65 g/L, 22 mM) (CRC, 2004; Miller and Witt, 1929) but is considered a strong base ($pkb_1 = 2.43$, $pkb_2 = 1.41$) (CRC, 2004). All measured Ca concentrations are below 5 mM (200 mg/L), which is below the solubility of $Ca(OH)_2$. It is difficult to estimate the dissolution kinetics, but it should be noted that the model wines analysed should be at equilibrium because, after separation from the ceramics, the model wine was kept in a flame-sealed tube at a controlled temperature for quite a very long period (from 16 months for the first samples to several weeks for the last ones). We can, therefore, assume that all available calcium hydroxide present in the model wine is dissolved and dissociated, in particular for the first experiments with small contact times (< 10 hours) where no precipitation or solid phase was observed. According to Eq. (3), the dissociation of calcium hydroxide should produce an increase in the pH of the model wine, as observed in Figure 4.

$$Ca(OH)_2(s) \rightarrow Ca^{2+}(aq) + 2OH^{-}(\text{aq}). \qquad (3)$$

Assuming a total dissociation of the base, for the first samples, the pH shift from 2.35 to 2.5 would correspond to a consumption of 1.3 mM of H_3O^+, which results from the dissociation of 0.65 mM of $Ca(OH)_2$ (corresponding to 26 mg/L of Ca^{2+}). When the pH reaches 7, the same calculation gives a dissociation of 2.2 mM (corresponding to 88 mg/L of Ca^{2+}) of $Ca(OH)_2$. It is reassuring to observe that despite the rough approximations, the estimated values are of the same order as the concentrations measured by ICP-AES.

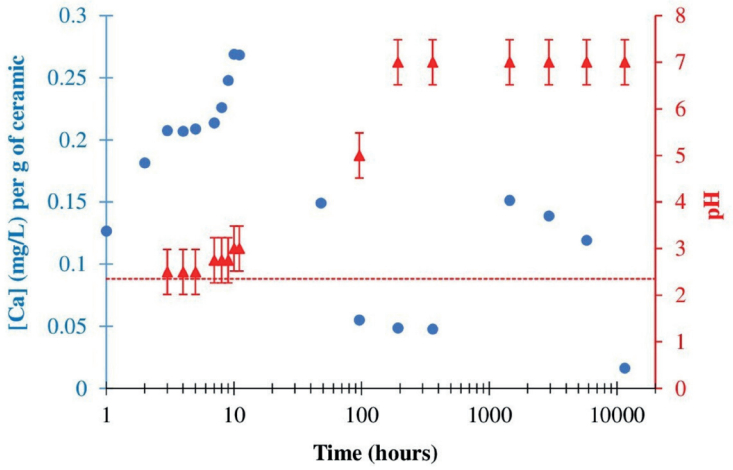


FIGURE 4. Blue circles: evolution of the Calcium concentration in model wine measured by ICP-AES (in mg/L per g of ceramic) versus the contact time between the model wine and the ceramic (model wine subtracted).

Red triangles: evolution of the pH. Due to the small volumes of model wine available, measurements were done by pouring a few drops of model wine onto pH indicator strips, which are subject to significant uncertainties estimated at ± 0.5 and reported by error bars. The dotted line corresponds to the pH of the starting model wine (2.35).

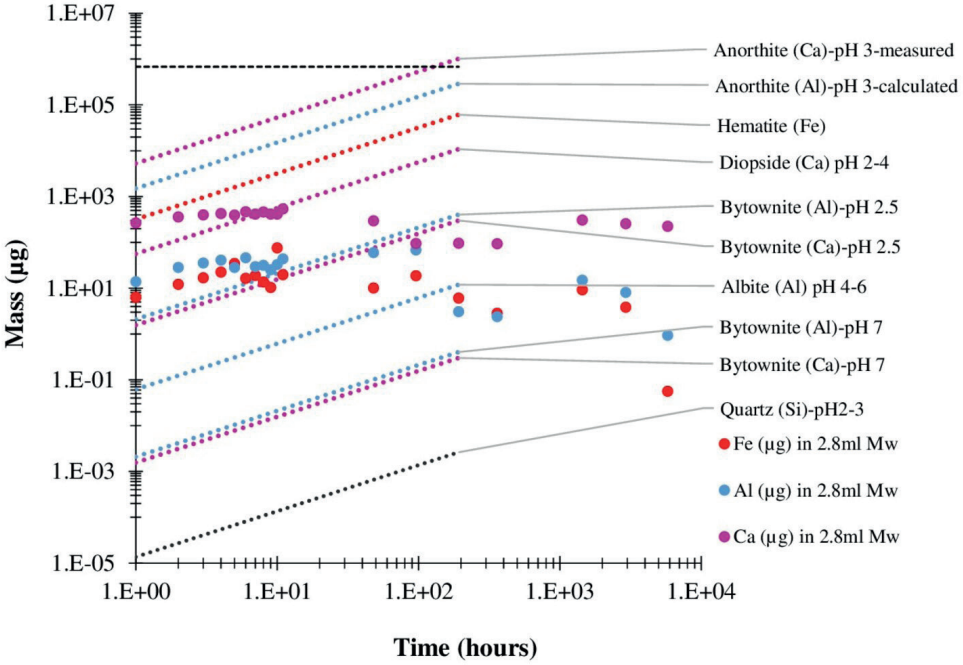


FIGURE 5. The mass of elements (µg) released from one tablet, measured in 2.8 mL of model wine by ICP-AES (full circles).

Simulated dissolution from literature data of an equivalent tablet (same surface area, average mass of 679 mg) are reported with dotted lines. The upper horizontal dashed black line figures the level corresponding to a mass of 679 mg.

Albeit the estimations for the first samples (26 mg/L) present the maximum discrepancy with the observed values (from 80 to 200 mM), it might be easier to discuss it since no precipitation or solid phase was observed for the first contact times, and the pH remained fairly stable. The simplest explanation for the underestimation of calcium concentration would be that more Ca is dissolved from other mineral sources. XRD revealed the presence of other calcium-containing-minerals in the ceramic: diopside ($CaMgSi_2O_6$), gehlenite ($Ca_2Al(AlSi)O_7$), but also plagioclase (labradorite ($Ca_{0.6}Na_{0.4}(Al_{1.6}Si_{2.4})O_8$), bytownite ($Ca_{0.8}Na_{0.2}(Al_{1.6}Si_{2.4})O_8$) and anorthite ($CaAl_2Si_2O_8$)).

2.2. The dissolution of ceramic minerals in model wine

The dissolution of ceramics and minerals such as diopside, hematite, magnetite and anorthite has been studied by several researchers (Bennett *et al.*, 1988; Knauss *et al.*, 1993; Knauss and Wolery, 1986; Lüttge *et al.*, 1999; Torrent, 1987; Welch and Ullman, 1993). Most of these studies have focused on mineral dissolution mechanisms as a function of pH and temperature. It is worth mentioning that results from the literature review may reveal noticeable discrepancies in dissolution constants depending on surface area or particle size (Bennett *et al.*, 1988; Bragança and Bergmann, 2006).

TABLE 2. Dissolution constant (K_d measured at 25 °C of some minerals identified in the ceramic. The reported values are generally obtained by a flow experiment. Quartz is given for comparison. ***I*** stands for low (not measured) pH. Dissolutions constants in bold were used for the calculations in Figure 5.

Mineral	Formula	pH	K_d (mol cm^{-2} s^{-1})	Reference
Anorthite	$CaAl_2Si_2O_8$	3	**$2.7\ 10^{-12}$**	Lüttge *et al.* (1999)
Bytownite	$Ca_{0.8}Na_{0.2}(Al_{1.6}Si_{2.4})O_8$	2–3	**10^{-12}**	Welch and Ullman (1993)
		7	**10^{-15}**	
Diopside	$CaMgSi_2O_6$	2–3	**$2.9\ 10^{-14}$**	Knauss *et al.* (1993)
Albite	$NaAlSi_3O_8$	4	**$4.7\ 10^{-17}$**	Knauss and Wolery (1986)
		6	$4.6\ 10^{-17}$	
Hematite	Fe_2O_3	*I*	**$5.8\ 10^{-14}$**	Torrent (1987)
Iron (III) hydroxide	$Fe(OH)_3$	4–6	10^{-13}	Deng (1997)
Quartz	SiO_2	2–3	**$3.6\ 10^{-17}$**	Bennett *et al.* (1988)

Some of these dissolution rates from the literature for a few minerals are given in Table 2. Figure 5 compares the elemental dissolution (Figure 3) with the simulation of the mineral dissolution according to Table 2. For the simulation, a hypothetical tablet with a mass of 679 mg made of 100 % of the mineral is considered. Figure 5 shows that the measured amount of dissolved element in the model wine is consistent with the dissolution constants reported in the literature. For example, a tablet of anorthite with the same surface area as the ceramic tablet can dissolve at 25 °C, pH 3, in one hour, up to 5.28 mg Ca. Compared to the amount of calcium (0.266 mg) measured after one hour of contact of the ceramic with the model wine, this suggests that if 5 % of the ceramic is anorthite (homogeneously distributed), this would be sufficient to produce the amount of calcium observed in the model wine (193 mg/L).

In addition, it is worth noting that Qin *et al.* (2016), using a very similar material (ceramsites), have evidenced that in conjunction with calcium release from calcium hydroxide, minerals (like gehlenite and anorthite) are also important dissolution sources for calcium. The results of Qin *et al.* (2016) need to be further compared to our results, and a detailed analysis of the calcium dissolution during the first hours may be engaged. They have studied the release of Ca^{2+} and OH^- from ceramsites containing anorthite and gehlenite prepared from waste lime mud. Qin *et al.* have modelled (at initial pH 6.5) the dissolution of Ca^{2+} by an Avrami law (fixing the Avrami constant n to 0.9019):

$$\frac{C(t)}{Cmax} = x = 1 - e^{-k\,t^n}, \qquad (4)$$

where k is the kinetic constant, n is the characteristic constant of the solid (Avrami constant), t is the time, x is the fractional conversion, $(C(t)$ is the concentration at time t and $Cmax$ is the maximal concentration).

They obtained kinetic coefficients from 0.0077 to 0.0125 min^{-n}. Figure 6 reports the fits of the concentration evolution of some elements according to Eq. (4), and the numerical results for the most abundant nuclei are reported in Table 3. Most elements seem to have the same kinetic constants (around 0.017), indicating a homogenous dissolution. Potassium and, to a lesser extent, sodium (but the incertitude is relatively large) reveal a lower k value. This apparent decrease in the kinetic constant could be associated with the precipitation of potassium bitartrates occurring during more than 16 months of storage of the model wines with ceramic tablets (before ICP-AES analyses) (Coulter *et al.*, 2015).

It is worth noting that in the experiments, the ratio of the model wine volume over the ceramic surface in contact with the wine ($R_{V/S}$) is less than 10 mm, which has to be compared with real containers. For example, $R_{V/S}$ is 15.7 mm for a Bordeaux-type bottle (0.75 L), 128 mm for a Bordeaux barrel (225 L) and 186 mm for an antic Armenian pithos (660 L) (Hovhannisyan *et al.*, 2017; p. 102, Fig. 138). For comparison between different containers, the dissolution rate should be scaled accordingly to the $R_{V/S}$ ratio.

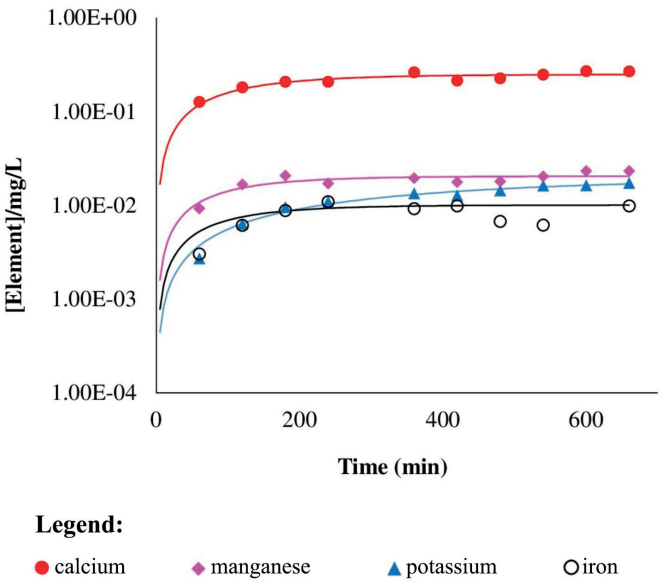


FIGURE 6. Refinement with an Avrami law: $C(t) = Cmax\left(1 - e^{-k\,t^n}\right)$ of the dissolution of calcium, manganese, potassium and iron during the first 12 hours of contact with a model wine. The concentrations are reported for 1 mg of ceramic.

TABLE 3. Parameter of the kinetic Avrami law for the most abundant dissolved nuclei. *Cmax* is reported for 1 mg of ceramic. The number in the bracket is the refinement error on the precedent digit (0.248(9) means 0.248 ± 0.009).

Element	(mg/L)/min.mg$_{ceram}$	K (t^n) n = 0.9019	Element	(mg/L)/min.mg$_{ceram}$	K (t^n) n = 0.9019
Ca	0.248(9)	0.016(3)	S	0.0047(2)	0.017(4)
Na	0.037(8)	0.010(7)	Sr	0.00072(2)	0.015(2)
K	0.021(2)	0.0049(7)	Mn	0.00028(2)	0.018(5)
Mg	0.0204(9)	0.018(4)	Zn	0.00024(7)	0.01(1)
Al	0.019(2)	0.017(7)	V	0.00011(1)	0.023(8)
Fe	0.010(2)	0.02(1)			

3. In situ analysis of the model wine in contact with the ceramic by TD NMR

The dissolution of the minerals from the ceramics can impact the characteristics of the wine. It may be responsible for a pH increase because of the acidic attack of the wine on the ceramic, and the dissolution of metallic elements (Fe, Cu…) may also promote the oxidation of ethanol. In practice, to minimise these possible effects, the surface of the ceramic is usually covered by a glassing formed during the firing of the ceramic at a higher temperature (sometimes with the preparation of the surface) (Zhang and Zhang, 2014), or traditionally, by an organic layer applied after firing (beeswax, pine pitch) (Barisashvili, 2011; Romanus *et al.*, 2009). The effect of a beeswax coating is illustrated by time-domain NMR measurement. Time domain NMR has the advantage of following the kinetic of dissolution in situ and, additionally, sheds light on the complex physicochemical evolution occurring in wine in the presence of a ceramic.

3.1. Contact of the ceramic with hydroalcoholic and tartaric solutions

The analysis of the proton spin–lattice relaxation in wine and hydroalcoholic solutions has been reported elsewhere (Bodart *et al.*, 2020; Bodart *et al.*, 2022), and Figure 7 shows the effect of the immersion of a ceramic in water, hydroalcoholic solution and tartaric acid solution. The physical act of immersion does not change the relaxation rate of the solution, as shown by the relaxation rate of the water protons from water and hydroalcoholic solution in contact with a ceramic. However, when the solution is acidic (tartaric acid solution), the relaxation rate increases rapidly as a result of an acidic attack of the ceramic, which releases some paramagnetic elements that enhance the relaxation rate.

3.2. Contributions of released paramagnetic elements to the proton relaxation rate of the model wine

ICP-AES has shown that the dissolution of the ceramic is susceptible to releasing all types of elements present in the ceramic. Amongst them, paramagnetic nuclei are of prime importance for the interpretation of TD-NMR experiments because they are responsible for the generally dominant dipolar paramagnetic relaxation mechanisms of the water protons of the solutions (Solomon, 1955). Interpretation of relaxograms can be difficult because of the variety of paramagnetic elements present in the model wine (Cd, Co, Cr, Cu, Fe, Mn, Mo, Ni, Ti and V) that have distinct relaxivity (i.e., the "power of relaxation" of paramagnetic nuclei on water protons, defined in solution as the ratio of the proton relaxation rate over the concentration of the paramagnetic element, Supplementary data, Table S3) (Bertini *et al.*, 2017). However, in conjunction with the concentration of the element determined by ICP-AES, it is possible to estimate an

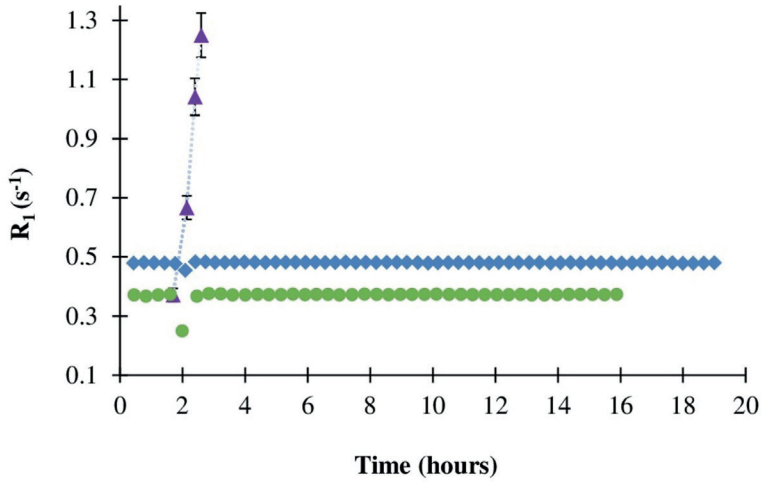


FIGURE 7. The relaxation rate of water (green circles), hydroalcoholic solution (blue diamonds) 12 % v/v, and tartaric acid solution (purple triangles) before (up to 2 hours) and after contact (after 2 hours) with ceramic.

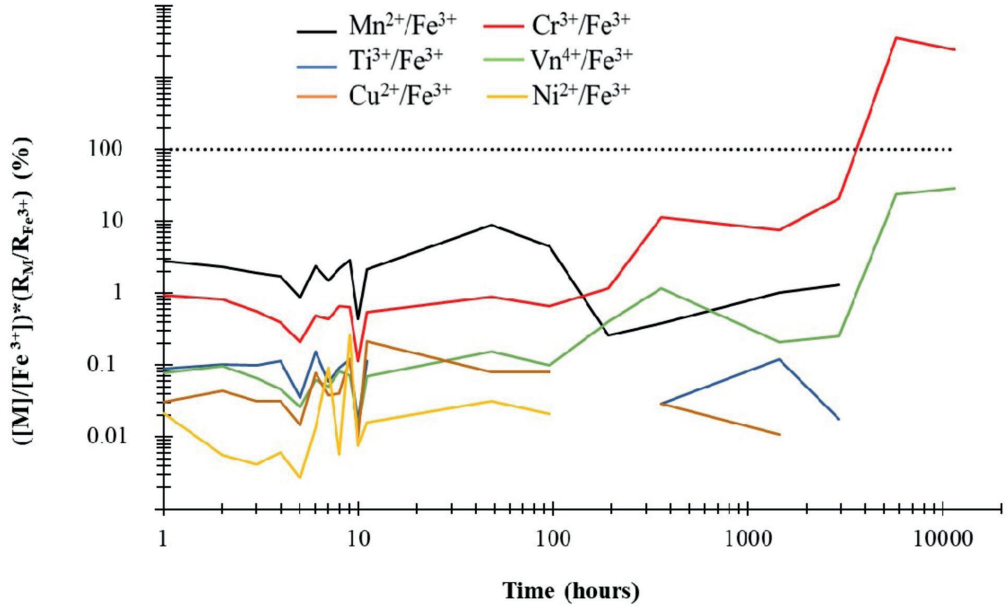


FIGURE 8. Ratios (in percent) of paramagnetic ions concentration with respect to the Fe concentration (extracted for ICP-AES data) *versus* ageing time, with ponderations relative to their relaxivity (Supplementary data, Table S2). Element concentrations from the model wine were subtracted. It is assumed that all elements are in the reported oxidation states. The horizontal dotted black line represents the calculated quantity for iron (100 %).

effective contribution of the paramagnetic element present in the model wines to the ^{1}H relaxation rate of the water molecules of the model wine (Figure 8).

Figure 8 reveals that under our experimental conditions, Fe^{3+} (dotted black line) is the main source of relaxation. The second contribution is Mn^{2+} (continuous black line) which has a maximum contribution (8.8 %) at t = 48 h. All other paramagnetic elements would contribute less than one-hundredth of the Fe^{3+} contribution. When the ratios become greater than 1, in particular for chromium and vanadium at long times, it is associated with a decrease in the iron concentration in the solution because of iron precipitation, whilst chromium and vanadium do not form solids.

Additionally, for the interpretation of the relaxogram, it is important to consider that the ^{1}H relaxation rate of water molecules in the model wine (R_1) is linearly dependent on the concentration of the paramagnetic element:

$$R_1 = R_0 + r_M[M], \qquad (5)$$

where R_0 is the relaxation rate of the solution without a paramagnetic element. r_M and $[M]$ are the relaxivity and the concentration of the paramagnetic element M, respectively. Figure S2 in Supplementary data reports the corresponding titration curve of Fe^{3+} in the model wine. The linear regression is numerically given by

$$R_1 = 0.478(3) + 0.065(1)[Fe^{3+}], \qquad (6)$$

where R_1 is expressed in s^{-1} and the concentration in mg/L (numbers in brackets are the incertitude given by the linear regression on the previous digit).

3.3. Iron dissolution

For comparison, Figure 9 reports the measured iron concentrations by ICP-AES and TD NMR techniques (a discussion of the relaxogram is reported in Section 3.4). For the first few hours, despite significant differences between the methods, the measured concentrations were fairly consistent. The equivalent Fe^{3+} concentrations measured by TD NMR are slightly higher than the concentrations measured by ICP-AES. Besides the possible variability between ceramic tablets, this overestimation could be attributed to the contribution of other paramagnetic ions to the relaxation rate of water molecules. For the comparison over long contact times, there are two major aspects to be considered: (i) unlike TD NMR, ICP-AES is not an in situ experiment and even if the model wine was in contact for 100 hours with the ceramics, for example, the ICP-AES measurements were performed more than 16 months later. The model wine, which was kept under controlled conditions in a sealed bulb, had a long period of time to evolve and reach an equilibrium state over the formation of various solid tartrates. (ii) with respect to the relaxogram, for long periods of time, the dissolved dioxygen concentration decreases (e.g., because of ethanol oxidation), leading to a reduction of ferric to ferrous ions, which are significantly less effective relaxation agents and giving low relaxations rate for the model wine.

3.4. Relaxograms of model wine after coating the ceramic tablets with beeswax

Figure 10 compares the relaxogram of ceramic tablets uncovered or covered with one or two layers of beeswax. It displays two vertical axes, the measured relaxation rates on the right and its conversion to an equivalent Fe^{3+} concentration on the left, according to Eq. (6).

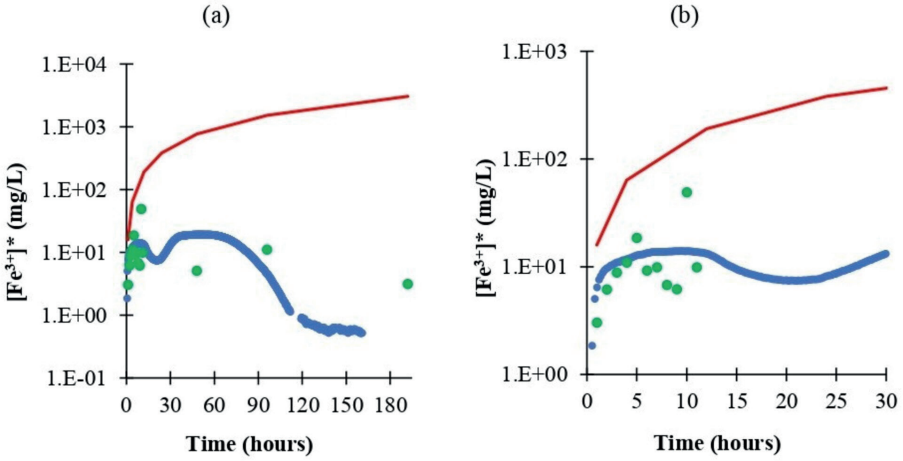


FIGURE 9. (a) Comparison of the equivalent ferric ion concentration calculated from the relaxogram (blue) and the ICP measurement (green). Statistics performed on all the ceramic tablets used for the ICP experiment give an average mass of 68050 mg, V_{wine} = 2.8 mL, V_{hs}/V_{wine} = 17 and $R_{V/S}$ = 7.34 mm. The solid red line indicates the theoretical labile iron resulting from the dissolution of hematite (estimated as 5 % of the mass of the ceramic). (b) is an expansion of (a).

First of all, it is necessary to discuss the relaxogram of the uncoated ceramic. Relaxograms of model wine in contact with a ceramic are rich in various information but may be complex to interpret; a detailed description is beyond the scope of this article and is reported to another one. Nevertheless, one can consider that the relaxation rate of water molecules depends on (i) the ratio of the volume of model wine over the surface of the ceramic, (ii) the amount of available dioxygen (dissolved and in the headspace), (iii) the pH of the solution. When the ceramic is immersed in the model wine, there is an immediate dissolution leading to the release (among many other elements) of Fe^{3+} from the dissolution of hematite, that is estimated to be 5 % of the ceramic. This induces a sharp increase in relaxation up to ~10 hours when the first maximum is reached. The dissolution of Fe^{3+} does not stop or decrease at 10 hours, but it continues and will decrease when the pH of the solution increases sufficiently. However, a decrease in the relaxation rate is observed with a minimum of 25 hours. A possible explanation could be attributed to the reduction of Fe^{3+} to iron Fe^{2+} (ferrous ions are significantly less effective as a relaxing agent than ferric ions, Supplementary data, Table S3, (Bodart *et al.*, 2020)). This would result in a decrease in the dissolved dioxygen concentration in the solution because of oxygen consumption in the solution through the oxidation of ethanol (catalysed by iron and other metals). However, this decrease is transitory because there are competitive reactions between the dissolution of dioxygen from the headspace into the solution, the dissolution of dioxygen resulting in the dissolution of the minerals composing the ceramic and oxidation reactions. After 25 hours, the relaxation rate increases again because of the continuous dissolution of Fe^{3+} and because of a slowing down of the dioxygen consumption in the solution. However, a plateau is reached at ~ 40 hours, and the relaxation rate starts to continuously decrease down to a value slightly higher than the relaxation rate of pure model wine because of (i) the slowing down of the dissolution because of the pH increase, (ii) the appearance of solid phases that can precipitate iron and (iii) a significant decrease in dioxygen in the solution and a reduction of paramagnetic metals.

However, the main purpose of Figure 10 is to compare the evolution of the relaxation rate of the ceramic with or without a coating. It is clear that the coating of the ceramic with beeswax significantly decreases the amount of released Fe^{3+} (but also of all elements). At 30 hours, the relaxograms show that dissolution is decreased by at least a factor of 4 or 170 if the ceramic is coated with one or two beeswax layers, respectively. Over the course of one year of contact of the coated ceramics with model wines, changes were observed related to both the colour of the model wine and the texture of the beeswax (Supplementary data, Figure S3). After three months, the samples coated with one layer of beeswax turned yellow but remained transparent, and the beeswax texture was slightly damaged. It should also be noted that no yellow or white precipitates or crystals were formed, which is typically observed with uncoated samples. A year later, the model wine in contact with the one-layer coated ceramic became hazy, and the texture of the beeswax continued to deteriorate. In the samples coated with two layers of beeswax and beeswax alone in the model wine, none of these changes (crystallisation, precipitation, haze formation, change in colour) were observed. This allows one to conclude that the changes that occur in the sample with one layer of beeswax are associated with the dissolution of the ceramic. This means that, at least for the reported period of time, an appropriate coating (in our case, with two layers) can strongly limit the acidic attack of the model wine on the ceramic, the migration of elements and the increase in pH.

CONCLUSION

ICP-AES analyses showed that a ceramic container could be easily deteriorated by the model wine it contains through an acidic attack, which dissolves the ceramic elements in the model wine. There is homogeneous dissolution of the minerals forming

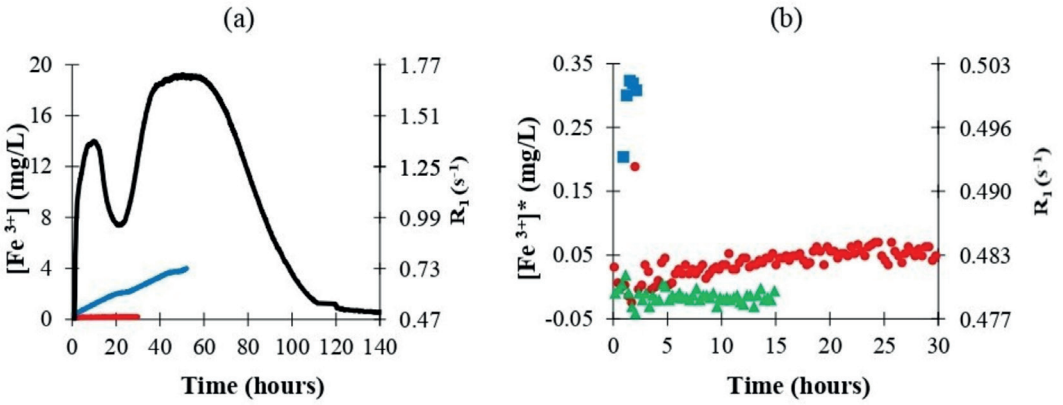


FIGURE 10. (a) Relaxograms of model wines in contact with beeswax-coated and non-coated ceramics. The black curve is the relaxogram of a non-coated ceramic (V_{wine} = 500 µL, $R_{V/S}$ = 5.2 mm, V_{hs}/V_{wine} ~ 17). The blue curve represents the relaxation rate of the model wine in contact with a ceramic coated by one layer of beeswax; the red curve is the relaxogram of the model wine in contact with a ceramic tablet coated with two layers of beeswax (V_{wine} = 700 µL, $R_{V/S}$ ~ 10 mm, V_{hs}/V_{wine} ~ 12). (b) is an expansion of (a) with the relaxogram of beeswax immersed in model wine (green triangles).

the ceramic consistent with the dissolution of the ceramic in acid water reported in the literature. This dissolution is concomitant with a significant increase in pH. Time domain NMR focused on the measurement of the ^1H relaxation time of water molecules in model wines, allowed to indirectly target the evolution of the Fe^{3+} concentration in the model wine in in situ experiments. It showed that the coating of the ceramic with beeswax could reduce the dissolution of the ceramic by at least a factor of 4 for one-layer coated or by a factor of 170 for two layers of coated ceramic.

ACKNOWLEDGEMENTS

Dr. Igor Bezverkhyy (Laboratoire Interdisciplinaire Carnot de Bourgogne, Université de Bourgogne) is thanked for performing BET measurements. Dr. Jean-Marc Dachicourt (École supérieure d'ingénieurs numérique et matériaux (ESIREM)) is thanked for the XRF measurements The authors thank the DIVVA platform (Institut Agro Dijon, Universite de Bourgogne) for the access Bruker minispec. C.F. and S.V. acknowledge financial support from the European Union (ERDF) and Région Nouvelle Aquitaine. This work is part of the project VALVIGNE (2020–2022, SYNERGIE BG0027582) supported by the conseil régional Bourgogne Franche Comté and the European Union through the FEDER—FSE Bourgogne 2014–2020 program.

REFERENCES

Aceto, M., Abollino, O., Bruzzoniti, M. C., Mentasti, E., Sarzanini, C., & Malandrino, M. (2002). Determination of metals in wine with atomic spectroscopy (flame-AAS, GF-AAS and ICP-AES); a review. *Food Additives and Contaminants*, *19*(2), 126–∑133. https://doi.org/10.1080/02652030110071336

Barisashvili, G. (2011). *Making Wine in Qvevri—A Unique Georgian Tradition*. Www.Kvevri.Org. Retrieved February 23, 2023, from www.kvevri.org/wp-content/uploads/2018/03/Making-Wine-in-Qvevri-a-Unique-Georgian-Tradition.pdf

Bennett, P. C., Melcer, M. E., Siegel, D. I., & Hassett, J. P. (1988). The dissolution of quartz in dilute aqueous solutions of organic acids at 25°C. *Geochimica et Cosmochimica Acta*, *52*(6), 1521–1530. https://doi.org/10.1016/0016-7037(88)90222-0

Bertini, I., Luchinat, C., Parigi, G., & Ravera, E. (2017). *NMR of paramagnetic molecules: Applications to metallobiomolecules and models* (Second edition). Elsevier. https://doi.org/10.1016/C2013-0-18690-4

Bodart, P. R., Batlogg, A., Ferret, E., Rachocki, A., Knapkiewicz, M., Esoyan, S., Hovhannisyan, N., Karbowiak, T., & Gougeon, R. D. (2022). Analysis of the Proton Spin–Lattice Relaxation in Wine and Hydroalcoholic Solutions. *Food Analytical Methods*, *15*(2), 266–275. https://doi.org/10.1007/s12161-021-02118-w

Bodart, P. R., Rachocki, A., Tritt-Goc, J., Michalke, B., Schmitt-Kopplin, P., Karbowiak, T., & Gougeon, R. D. (2020). Quantification of manganous ions in wine by NMR relaxometry. *Talanta*, *209*, 120561. https://doi.org/10.1016/j.talanta.2019.120561

Bragança, S. R., & Bergmann, C. P. (2006). Effect of Quartz of Fine Particle Size on Porcelain Properties. *Materials Science Forum*, *530–531*, 493–498. https://doi.org/10.4028/www.scientific.net/MSF.530-531.493

Cabrita, M. J., Martins, N., Barrulas, P., Garcia, R., Dias, C. B., Pérez-Álvarez, E. P., Costa Freitas, A. M., & Garde-Cerdán, T. (2018). Multi-element composition of red, white and palhete amphora wines from Alentejo by ICPMS. *Food Control*, *92*, 80–85. https://doi.org/10.1016/j.foodcont.2018.04.041

Cacho, J., Castells, J. E., Esteban, A., Laguna, B., & Sagristá, N. (1995). Iron, Copper, and Manganese Influence on Wine Oxidation. *American Journal of Enology and Viticulture*, *46*(3), 380–384. https://doi.org/10.5344/ajev.1995.46.3.380

Coleman, R. E., Boulton, R. B., & Stuchebrukhov, A. A. (2020). Kinetics of autoxidation of tartaric acid in presence of iron. *The Journal of Chemical Physics*, *153*(6), 064503. https://doi.org/10.1063/5.0013727

Coulter, A. D., Holdstock, M. G., Cowey, G. D., Simos, C. A., Smith, P. A., & Wilkes, E. N. (2015). Potassium bitartrate crystallisation in wine and its inhibition: Cold stability. *Australian Journal of Grape and Wine Research*, *21*, 627–641. https://doi.org/10.1111/ajgw.12194

CRC (2004). *CRC handbook of chemistry and physics: A ready-reference book of chemical and physical data* (D. R. Lide, Ed.; 85. ed). CRC Press.

Criado, Y. A., Alonso, M., & Abanades, J. C. (2014). Kinetics of the $CaO/Ca(OH)_2$ Hydration/Dehydration Reaction for Thermochemical Energy Storage Applications. *Industrial & Engineering Chemistry Research*, *53*(32), 12594–12601. https://doi.org/10.1021/ie404246p

Danilewicz, J. C. (2016). Fe(II):Fe(III) Ratio and Redox Status of White Wines. *American Journal of Enology and Viticulture*, *67*(2), 146–152. https://doi.org/10.5344/ajev.2015.15088

Danilewicz, J. C. (2018). [Fe(III)]:[Fe(II)] Ratio and Redox Status of Red Wines: Relation to So-Called "Reduction Potential". *American Journal of Enology and Viticulture*, *69*(2), 141–147. https://doi.org/10.5344/ajev.2017.17081

Deng, Y. (1997). Effect of pH on the Reductive Dissolution Rates of Iron(III) Hydroxide by Ascorbate. *Langmuir*, *13*(6), 1835–1839. https://doi.org/10.1021/la9607013

Elias, R. J., & Waterhouse, A. L. (2010). Controlling the Fenton Reaction in Wine. *Journal of Agricultural and Food Chemistry*, *58*(3), 1699–1707. https://doi.org/10.1021/jf903127r

Gil i Cortiella, M., Ubeda, C., Covarrubias, J. I., Laurie, V. F., & Peña-Neira, Á. (2021). Chemical and Physical Implications of the Use of Alternative Vessels to Oak Barrels during the Production of White Wines. *Molecules*, *26*(3), 554. https://doi.org/10.3390/molecules26030554

Gougeon, R. D., Lucio, M., Frommberger, M., Peyron, D., Chassagne, D., Alexandre, H., Feuillat, F., Voilley, A., Cayot, P., Gebefügi, I., Hertkorn, N., & Schmitt-Kopplin, P. (2009). The chemodiversity of wines can reveal a metabologeography expression of cooperage oak wood. *Proceedings of the National Academy of Sciences*, *106*(23), 9174–9179. https://doi.org/10.1073/pnas.0901100106

Guerrini, L., Maioli, F., Picchi, M., Zanoni, B., Parenti, A., & Canuti, V. (2022). Kinetic modeling of a Sangiovese wine's chemical and physical parameters during one-year aging in different tank materials. *European Food Research and Technology*, *248*(6), 1525–1539. https://doi.org/10.1007/s00217-022-03982-4

Harutyunyan, M., Viana, R., Granja-Soares, J., Martins, M., Ribeiro, H., & Malfeito-Ferreira, M. (2022). Adaptation of Ancient Techniques to Recreate 'Wines' and 'Beverages' Using Withered Grapes of Muscat of Alexandria. *Fermentation*, *8*(2), 85. https://doi.org/10.3390/fermentation8020085

Hovhannisyan, N. A., Yesayan, A. A., Bobokhyan, A., Dallakyan, M. V., Hobosyan, S., & Gasparyan, B. Z. (2017). *Armenian vine and wine*.

Johnson, K., Zhang, Y., & Trela, B. (2013). Evaluation of Qvevri in Winemaking. *64th ASEV National Conference*, 128–129. Retrieved February 23, 2023, from http://www.asev.org/sites/main/files/file-attachments/2013technicalabstracts.pdf?1410302529

Knauss, K. G., Nguyen, S. N., & Weed, H. C. (1993). Diopside dissolution kinetics as a function of pH, CO_2, temperature, and time. *Geochimica et Cosmochimica Acta*, *57*(2), 285–294. https://doi.org/10.1016/0016-7037(93)90431-U

Knauss, K. G., & Wolery, T. J. (1986). Dependence of albite dissolution kinetics on ph and time at 25°c and 70°c. *Geochimica et Cosmochimica Acta*, *50*(11), 2481–2497. https://doi.org/10.1016/0016-7037(86)90031-1

Lüttge, A., Bolton, E. W., & Lasaga, A. C. (1999). An interferometric study of the dissolution kinetics of anorthite; the role of reactive surface area. *American Journal of Science*, *299*(7–9), 652–678. https://doi.org/10.2475/ajs.299.7-9.652

MacNeil, K. (2015). *The wine bible* (Revised Second Edition). Workman Publishing Company.

Martínez-Gil, A., Del Alamo-Sanza, M., & Nevares, I. (2022). Evolution of red wine in oak barrels with different oxygen transmission rates. Phenolic compounds and colour. *LWT*, *158*, 113133. https://doi.org/10.1016/j.lwt.2022.113133

McGovern, P., Jalabadze, M., Batiuk, S., Callahan, M. P., Smith, K. E., Hall, G. R., Kvavadze, E., Maghradze, D., Rusishvili, N., Bouby, L., Failla, O., Cola, G., Mariani, L., Boaretto, E., Bacilieri, R., This, P., Wales, N., & Lordkipanidze, D. (2017). Early Neolithic wine of Georgia in the South Caucasus. *Proceedings of the National Academy of Sciences*, *114*(48). https://doi.org/10.1073/pnas.1714728114

Miller, L. B., & Witt, J. C. (1929). Solubility of Calcium Hydroxide. *The Journal of Physical Chemistry*, *33*(2), 285–289. https://doi.org/10.1021/j150296a010

Montalvo, F. F., García-Alcaraz, J. L., Cámara, E. M., Jiménez-Macías, E., & Blanco-Fernández, J. (2021). Environmental impact of wine fermentation in steel and concrete tanks. *Journal of Cleaner Production*, *278*, 123602. https://doi.org/10.1016/j.jclepro.2020.123602

Nevares, I., & del Alamo-Sanza, M. (2021). Characterisation of the Oxygen Transmission Rate of New-Ancient Natural Materials for Wine Maturation Containers. *Foods*, *10*(1), 140. https://doi.org/10.3390/foods10010140

Nikolantonaki, M., Daoud, S., Noret, L., Coelho, C., Badet-Murat, M.-L., Schmitt-Kopplin, P., & Gougeon, R. D. (2019). Impact of Oak Wood Barrel Tannin Potential and Toasting on White Wine Antioxidant Stability. *Journal of Agricultural and Food Chemistry*, *67*(30), 8402–8410. https://doi.org/10.1021/acs.jafc.9b00517

Nikulshina, V., Gálvez, M. E., & Steinfeld, A. (2007). Kinetic analysis of the carbonation reactions for the capture of CO_2 from air via the $Ca(OH)_2$–$CaCO_3$–CaO solar thermochemical cycle. *Chemical Engineering Journal*, *129*(1–3), 75–83. https://doi.org/10.1016/j.cej.2006.11.003

Ohls, K., & Bogdain, B. (2016). History of inductively coupled plasma atomic emission spectral analysis: From the beginning up to its coupling with mass spectrometry. *Journal of Analytical Atomic Spectrometry*, *31*(1), 22–31. https://doi.org/10.1039/C5JA90043C

Qin, J., Yang, C., Cui, C., Huang, J., Hussain, A., & Ma, H. (2016). Ca^{2+} and OH^- release of ceramsites containing anorthite and gehlenite prepared from waste lime mud. *Journal of Environmental Sciences*, *47*, 91–99. https://doi.org/10.1016/j.jes.2016.03.013

Romanus, K., Baeten, J., Poblome, J., Accardo, S., Degryse, P., Jacobs, P., De Vos, D., & Waelkens, M. (2009). Wine and olive oil permeation in pitched and non-pitched ceramics: Relation with results from archaeological amphorae from Sagalassos, Turkey. *Journal of Archaeological Science*, *36*(3), 900–909. https://doi.org/10.1016/j.jas.2008.11.024

Sanchez-Garmendia, U., Iñañez, J. G., & Arana, G. (2021). Alterations and Contaminations in Ceramics Deposited in Underwater Environments: An Experimental Approach. *Minerals*, *11*(7), 766. https://doi.org/10.3390/min11070766

Serris, E., Favergeon, L., Pijolat, M., Soustelle, M., Nortier, P., Gärtner, R. S., Chopin, T., & Habib, Z. (2011). Study of the hydration of CaO powder by gas–solid reaction. *Cement and Concrete Research*, *41*(10), 1078–1084. https://doi.org/10.1016/j.cemconres.2011.06.014

Shackelford, J., & Shackelford, P. (2020). Ceramics in the wine industry. *International Journal of Ceramic Engineering & Science*, *3*. https://doi.org/10.1002/ces2.10073

Solomon, I. (1955). Relaxation Processes in a System of Two Spins. *Physical Review*, *99*(2), 559–565. https://doi.org/10.1103/PhysRev.99.559

Stanmore, B. R., & Gilot, P. (2005). Review—Calcination and carbonation of limestone during thermal cycling for CO2 sequestration. *Fuel Processing Technology*, *86*(16), 1707–1743. https://doi.org/10.1016/j.fuproc.2005.01.023

Torrent, J. (1987). The Reductive Dissolution of Synthetic Goethite and Hematite in Dithionite. *Clay Minerals - CLAY MINER*, *22*, 329–337. https://doi.org/10.1180/claymin.1987.022.3.07

Twede, D. (2002). Commercial Amphoras: The Earliest Consumer Packages? *Journal of Macromarketing*, *22*(1), 98–108. https://doi.org/10.1177/027467022001009

van Duynhoven, J., Voda, A., Witek, M., & Van As, H. (2010). Time-Domain NMR Applied to Food Products. In *Annual Reports on NMR Spectroscopy* (Vol. 69, pp. 145–197). Elsevier. https://doi.org/10.1016/S0066-4103(10)69003-5

Welch, S. A., & Ullman, W. J. (1993). The effect of organic acids on plagioclase dissolution rates and stoichiometry. *Geochimica et Cosmochimica Acta*, *57*(12), 2725–2736. https://doi.org/10.1016/0016-7037(93)90386-B

Weltman, P. (2018). *Why an Ancient Winemaking Technique Is Making a Comeback*. Daily.Sevenfifty.Com. Retrieved February 24, 2023, from https://daily.sevenfifty.com/why-an-ancient-technique-is-making-a-comeback/

Work, H. (2014). *Wood, whiskey and wine: A history of barrels*. Reaktion Books.

Zhang, X., & Zhang, H. (2014). *Research on Meiping in the Application of Chinese Traditional Wine Packaging:* International Conference on Education, Language, Art and Intercultural Communication (ICELAIC-14), Zhengzhou, Henan, China. https://doi.org/10.2991/icelaic-14.2014.120